Origin of coexisting large Seebeck coefficient and metallic conductivity in the electron doped $SrTiO_3$ and $KTaO_3$

Hidetomo Usui, Shinsuke Shibata,* and Kazuhiko Kuroki
Department of Applied Physics and Chemistry, The University of Electro-Communication, Chofu, Tokyo 182-8585, Japan
(Received 1 February 2010; revised manuscript received 14 April 2010; published 25 May 2010)

We study the origin of the large Seebeck coefficient despite the metallic conductivity in the La-doped $SrTiO_3$ and Ba-doped $KTaO_3$. We calculate the band structure of $SrTiO_3$ and $KTaO_3$, from which the Seebeck coefficient is obtained using the Boltzmann's equation. We conclude that the multiplicity of the t_{2g} bands in these materials is one major origin of the good thermoelectric property in that when compared at a fixed total number of doped electrons, the Seebeck coefficient and thus the power factor are larger in multiple band systems than in single band ones because the number of doped electron bands *per band* is smaller in the former. We also find that the second-nearest-neighbor hopping integral, which generally has negative values in these materials and works destructively against the Seebeck effect, is nearly similar between $KTaO_3$ and $SrTiO_3$ despite the larger bandwidth in the former. This can be another factor favorable for thermopower in the Ba-doped $KTaO_3$.

DOI: 10.1103/PhysRevB.81.205121 PACS number(s): 72.15.Jf, 71.20.−b

I. INTRODUCTION

The discovery of the large Seebeck coefficient in Na_xCoO_2 (Ref. 1) and the findings in cobaltates/cobaltites[2–6] and rhodates[7,8] that followed have brought up an interesting possibility of finding good thermoelectric materials among the oxides that have relatively high (metallic) conductivity. These cobaltates and rhodates are materials where holes are doped into the d^6 configuration, namely, the electron configuration where the t_{2g} bands are fully filled. On the other hand, there is another class of t_{2g} transition-metal oxides where relatively good thermoelectric properties are obtained, namely, the electron doped materials such as $SrTiO_3$.[9,10] When Sr is partially replaced by La in $SrTiO_3$, electrons are doped in the originally d^0 configuration. This material exhibits large Seebeck coefficient despite showing metallic conductivity, and the power factor, i.e., the Seebeck coefficient squared times the conductivity, is comparable to that of Bi_2Te_3. Quite recently, good thermoelectric properties have also been observed in Ba-doped $KTaO_3$.[11] This is another t_{2g} oxide, where electrons are doped into the originally d^0 configuration, but is a $5d$ system as compared to the $3d$ in $SrTiO_3$. Here again, relatively large Seebeck coefficient is observed despite the metallic conductivity.

Theoretically, there have been several approaches that explain the large Seebeck coefficient in oxides. From the first-principles band calculation studies, it has been pointed out that the narrowness of the band structure in Na_xCoO_2 and related rhodates is an important factor.[12,13] We have proposed that besides the width of the band, the shape of the band, which we call the "pudding-mold" type band, is important for the coexistence of the large Seebeck coefficient and the high conductivity in Na_xCoO_2 (Ref. 14) and related rhodates.[15,16] On the other hand, Koshibae *et al.*[17,18] derived a formula for the Seebeck coefficient in the T(temperature) $\rightarrow\infty$ limit, and pointed out that the orbital degeneracy originates large entropy, leading to the large Seebeck coefficient. In fact, for $KTaO_3$ due to the degeneracy of the t_{2g} orbitals, the possible applicability of this scenario has been pointed out.[11] On the other hand, the orbital/band multiplicity can enhance the figure of merit in a more conventional way in that the number of carriers for a fixed chemical potential positively correlates with the band multiplicity, as has been discussed theoretically.[16,19,20] In fact, the origin of the large Seebeck coefficient in doped $SrTiO_3$ has been discussed from this point of view in the experimental studies.[9,10] However, in the theoretical analysis of these studies, the band structure of $SrTiO_3$ has been assumed to be of the three dimensional, isotropic, nearly free electron type with a certain effective mass, while in reality this is not accurate due to the two-dimensional (despite the three dimensionality of the lattice), tight-binding nature of the $3d_{xy}$, d_{yz}, and d_{zx} bands.

In the present study, we theoretically study the origin of the large Seebeck effect in the electron doped t_{2g} materials. Our aim is to show, using first-principles calculation that *takes into account the actual band structure of the materials*, that the following mechanism is at work in these materials. Namely, when there are multiple (nearly) equivalent bands at the Fermi level, and the number of doped electrons *per band* is fixed, the Seebeck coefficient is essentially the same regardless of the number of bands, while the conductivity increases with the multiplicity of the bands thus resulting in an enhanced power factor. In other words, when the *total number of doped electrons* itself is fixed, the Seebeck coefficient and thus the power factor is larger for multiple band systems because the Fermi energy stays low. We also examine the effect of the band shape, and show that the second-nearest-neighbor hopping integral, which generally has negative values in these materials and work destructively against the Seebeck effect, is nearly similar between $KTaO_3$ and $SrTiO_3$ despite the larger bandwidth in the former. This can be another factor favorable for good thermoelectric properties in the Ba-doped $KTaO_3$.

II. FORMULATION

A. Boltzmann's equation approach

We first briefly summarize the Boltzmann's equation approach adopted in the present study.[13,20] In this approach, the Seebeck coefficient is given as

$$\mathbf{S} = \frac{1}{eT}\mathbf{K}_0^{-1}\mathbf{K}_1, \tag{1}$$

where $e(<0)$ is the electron charge, T is the temperature, tensors $\mathbf{K}_0$ and $\mathbf{K}_1$ are given by

$$\mathbf{K}_n = \sum_{\vec{k}} \tau(\vec{k})\vec{v}(\vec{k})\vec{v}(\vec{k})\left[-\frac{\partial f(\varepsilon)}{\partial \varepsilon}(\vec{k})\right][\varepsilon(\vec{k}) - \mu]^n. \tag{2}$$

Here, $\varepsilon(\vec{k})$ is the band dispersion, $\vec{v}(\vec{k}) = \nabla_{\vec{k}}\varepsilon(\vec{k})$ is the group velocity, $\tau(\vec{k})$ is the quasiparticle lifetime, $f(\varepsilon)$ is the Fermi distribution function, and μ is the chemical potential. Hereafter, we simply refer to $(\mathbf{K}_n)_{xx}$ as K_n, and $S_{xx} = (1/eT)(K_1/K_0)$ (for diagonal $\mathbf{K}_0$) as S. Using K_0, conductivity can be given as $\sigma_{xx} = e^2K_0 \equiv \sigma = 1/\rho$. As an input of the band structure in this calculation, we use the first-principles calculation as described below. $\tau(\vec{k})$ will be taken as an (undetermined) constant in the present study, so that it cancels out in the Seebeck coefficient, while the conductivity and thus the power factor has to be normalized by a certain reference.

B. Band calculation

$SrTiO_3$ and $KTaO_3$ have cubic perovskite structures. We use the experimentally determined lattice constants in the band calculation, which are $a = 3.90528$ Å for $SrTiO_3$ (Ref. 21) and $a = 3.9883$ Å for $KTaO_3$.[22] For $SrTiO_3$, we have obtained the band structure using the QUANTUM-ESPRESSO package.[23] In order to obtain a tight-binding model on which we can perform various analysis, we construct the maximally localized Wannier functions (MLWFs) (Ref. 24) for the outer energy window $0 < \epsilon_k - E_F < 5$ eV and for the inner windows $0 < \epsilon_k - E_F < 4$ eV, where ϵ_k is the eigenenergy of the Bloch states and E_F is the Fermi energy. These MLWFs, centered at Ti sites in the unit cell, have three orbital symmetries (orbital $1: d_{xy}$, $2: d_{yz}$, and $3: d_{zx}$). With these effective hoppings and on-site energies, the tight-binding Hamiltonian is obtained, and finally the Seebeck coefficient is calculated using Eq. (1). For $KTaO_3$, we have obtained the band structure using the WIEN2K package.[25] The Seebeck coefficient is calculated using the BOLTZTRAP code.[26]

III. CALCULATION RESULTS OF THE SEEBECK COEFFICIENT

In this section, we present the band calculation results and the calculation results of the Seebeck coefficient. The calculated band structures of $SrTiO_3$ and $KTaO_3$ are shown in Fig. 1. In both materials, there are three t_{2g} bands right above the Fermi level, and for $SrTiO_3$, the band structure of the three band tight-binding model is superposed to the original first-principles band. The band structure of the two materials look similar but the band width is wider for $KTaO_3$ due to the widely spread nature of the $5d$ orbitals.

The calculated Seebeck coefficient for the two materials is shown in Fig. 2 against the temperature at $x = 0.05$ and $x = 0.1$ for $SrTiO_3$ and $x = 0.009$ for $KTaO_3$. We have chosen these x to make comparison with the experiments.[9,11] Here

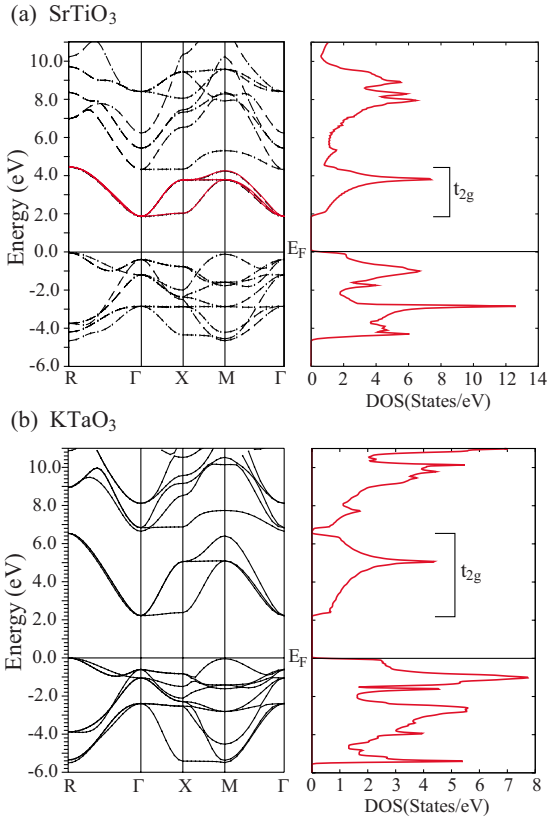

FIG. 1. (Color online) The band structure and the density of states of (a) $SrTiO_3$ and (b) $KTaO_3$. In (a), the black dotted lines are the original LDA calculation while the solid red lines are the bands of the tight-binding model obtained using the MLWFs. The labels in the Brillouin zone R, G, X, and M corresponds to (π, π, π), (0,0,0), $(\pi, 0, 0)$, and $(\pi, \pi, 0)$, in units of the lattice constant, respectively.

we take a rigid band approach and assume that the hole concentration n_h is equal to the La ($SrTiO_3$) and Ba ($KTaO_3$) content.

For $SrTiO_3$, the Seebeck coefficient at 300 K is $S(x = 0.05) = -87$ μV/K and $S(x = 0.1) = -58$ μV/K. Experimentally, the Seebeck coefficient at 300 K is $S(x = 0.05) = -147$ μV/K and $S(x = 0.1) = -88.7$ μV/K.[9] Thus the calculation result is somewhat reduced from the experimental result. The reason for this is probably due to the reduction in the bandwidth due to the strong correlation effect of the $3d$ orbitals. In fact, it has been known from the comparison between band calculations and the angle-resolved photoemission studies that the bandwidth of the $3d$ electron materials is generally reduced by a factor of about 2, and in fact taking this effect into account reproduces the experimental results of Na_xCoO_2 well.[14] If we calculate the Seebeck coefficient at 300 K by reducing the bandwidth by 50% from the bare local-density approximation (LDA) result, we get $S(x = 0.05) = -149$ μV/K and $S(x = 0.1) = -103$ μV/K [Fig. 2(a)], which are in fact fairly close to the experimental values.

As for $KTaO_3$, the calculation of the Seebeck coefficient at $x = 0.009$ gives $S(300\ \text{K}) = -160$ μV/K. This is roughly in agreement with the experimental result which is about -200 μV/K.[11] A reason why the bare LDA band structure

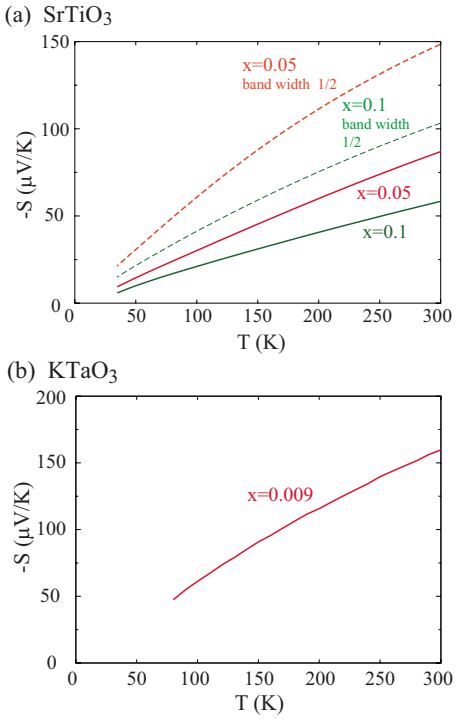

FIG. 2. (Color online) The calculated Seebeck coefficient for (a) $SrTiO_3$ and (b) $KTaO_3$ plotted as functions of temperature for various doping rate x. In (a), the solid lines are obtained using the original effective model while the dashed lines are obtained using a model where the bandwidth is halved.

gives good agreement with the experiments is because $KTaO_3$ is a $5d$ system, where the electron correlation effects are expected to be small compared to $3d$ systems such as $SrTiO_3$. In fact, for a number of rhodates, i.e., $4d$ systems, the Seebeck coefficient calculated from the bare LDA band structure gives fairly good agreement with the experiments.[13,15,16]

IV. EFFECT OF THE BAND MULTIPLICITY

Having found that the experimentally observed Seebeck coefficient is roughly reproduced within the first-principles band calculation+the Boltzmann's equation approach (with some additional consideration of band narrowing), we now explain why the Seebeck coefficient is large in these materials despite the relatively large conductivity. In other words, we seek for the origin of the large power factor $S^2\sigma$.

In the three orbital model, the Seebeck coefficient S_{xx} is given as

$$S_{xx} = \frac{1}{eT}\frac{K_1^{dxy} + K_1^{dyz} + K_1^{dzx}}{K_0^{dxy} + K_0^{dyz} + K_0^{dzx}}, \tag{3}$$

where K_n^{dij} stands for K_n of the $d_{ij}(i,j=x,y,z)$ orbital. From Eq. (2), the group velocity v_x^{dij} is the important factor in K_n. v^{dxy} is equal to v^{dzx} because $d(\varepsilon_{xy})/dx$ is equal to $d(\varepsilon_{zx})/dx$ so that $K_n^{dxy}=K_n^{dzx}$. Also, $K_n^{dyz}\sim 0$ because v^{dyz} is very small. So the Seebeck coefficient is

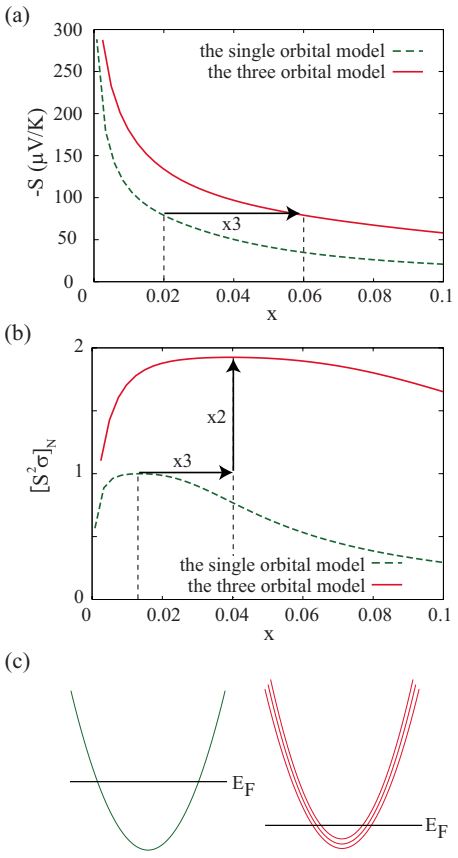

FIG. 3. (Color online) (a) The Seebeck coefficient and (b) the normalized power factor of the single orbital model (dashed green) and the three orbital models (solid red) as functions of the doping rate x at 300 K. (c) Schematic figure of how the Fermi energy differs between single and multiband systems.

$$S_{xx} \sim \frac{1}{eT}\frac{2K_1^{dxy}}{2K_0^{dxy}} = \frac{1}{eT}\frac{K_1^{dxy}}{K_0^{dxy}} = S_{xx}^{dxy}. \tag{4}$$

Namely, the total Seebeck coefficient is equal to the Seebeck coefficient of the d_{xy} single orbital system. On the other hand, the conductivity is

$$\sigma = e^2(K_0^{dxy} + K_0^{dyz} + K_0^{dzx}) \sim 2e^2K_0^{dxy} = 2\sigma^{dxy}. \tag{5}$$

Therefore, the power factor is

$$P_{xx} = \sigma S_{xx}^2 \sim 2\sigma^{dxy}(S_{xx}^{dxy})^2 = 2P_{xx}^{dxy}. \tag{6}$$

The left-hand side here is the power factor of the three orbital system while P_{xx}^{dxy} in the right-hand side is that of the d_{xy} single orbital system. Thus the multiplicity of the orbitals is advantageous for large power factor. Note that the comparison here between the three orbital and the single orbital systems is given for the same number of electrons *per band*. If we present this relation between the three and one orbital systems using the *doping concentration* x, it should be given as $S_{xx}(3x)=S_{xx}^{dxy}(x)$ and $P_{xx}(3x)=2P_{xx}^{dxy}(x)$.

In Fig. 3, we show the actual calculation result of the Seebeck coefficient and the power factor (normalized at $x=0.13$ of the single orbital model) of the t_{2g} three orbital model of $SrTiO_3$ and a single orbital model where only the

d_{xy} orbital is considered. It can be seen that the above relation is indeed satisfied. It is also worth noting that the doping dependence of the power factor is in striking agreement with the experimental observation (Fig. 3 in Ref. 9). From this figure, we can see that for a fixed doping concentration, both the Seebeck coefficient and the power factor is larger for multiorbital systems than in single orbital ones. This can intuitively be understood from Fig. 3(c), namely, the Fermi level tends to stay lower for systems with multiple bands for a fixed number of doped electrons, and lower Fermi level results in a large Seebeck coefficient, while the large number of electrons (due to the multiplicity of the bands) enhances the conductivity.[16] The present result suggests that the band multiplicity is at least one of the main reasons why the Seebeck coefficient is large despite the metallic conductivity. The orbital degeneracy has been considered as a factor to obtain good thermoelectric properties in the context of entropy[17,18] but we stress here that the present mechanism provides another way where the band multiplicity can play an important role.[16]

V. EFFECT OF THE BAND SHAPE

In the present materials, the density of states (DOS) *per band* is not so large around the Fermi level. This can roughly be understood in terms of the tight-binding model. Namely, the tight-binding model on a square lattice has electron-hole symmetry when only the nearest-neighbor hopping t_1 is considered. The introduction of the second-nearest-neighbor hopping t_2 breaks this electron-hole symmetry, and for t_{2g} systems, this hopping integral usually has a negative sign when writing down the Hamiltonian in the form $H=\Sigma_{ij}t_{ij}c_i^\dagger c_j$. When t_2 is negative, the density of states tends to be large in the upper half of the band and small in the lower half. This can actually be seen in the density of states shown in Fig. 1, where the t_{2g} bands has a DOS peak in the upper portion. In this sense, the effect of the so-called "pudding-mold-type" band,[14] where a flat portion of the band has to be present near the Fermi level, is not relevant to the present electron doped materials.[27] This can in fact be seen as follows. Since we have found that $S_{xx} \simeq S_{xx}^{dxy}$ (assuming same electron number per band) in the preceding section, we concentrate here on the d_{xy} single orbital model of $SrTiO_3$. In this model, the nearest- and second-nearest-neighbor hoppings of the MLWF tight-binding Hamiltonian are $t_1=-0.28$ eV and $t_2=-0.078$ eV. To see how t_2 affects the Seebeck coefficient, we vary t_2 while fixing $t_1=-0.28$ eV, and calculate the Seebeck coefficient at 300 K as shown Fig. 4(a). It is found that the smaller $|t_2|$ is, the larger the Seebeck coefficient. This is because the lower part of the band (where the Fermi level exists) become less dispersive as $|t_2|$ is decreased when t_2 is negative. This can be seen in the calculation of the DOS given in Fig. 4(b), namely, the DOS at the band bottom for $t_2=0$ eV is about twice larger than for $t_2=-0.13$ eV. Thus the negative value of t_2 (i.e., the band shape) in $SrTiO_3$ is not favorable for thermopower, and the good thermoelectric properties seem to come mainly from the multiplicity of the bands.

Conversely, materials having smaller $|t_2|$ with a similar band structure may give a larger Seebeck coefficient. From this viewpoint, we have also obtained the effective model for the titanates with different cations as given in Table I.[33] We find that $|t_2|$ is smaller for $BaTiO_3$ (and also slightly smaller for $PbTiO_3$) than for $SrTiO_3$. t_1, which directly affects the bandwidth, is also smaller in $BaTiO_3$. As shown in Fig. 5, we calculate the Seebeck coefficient for these materials using the effective models and find that $BaTiO_3$ has a larger value than

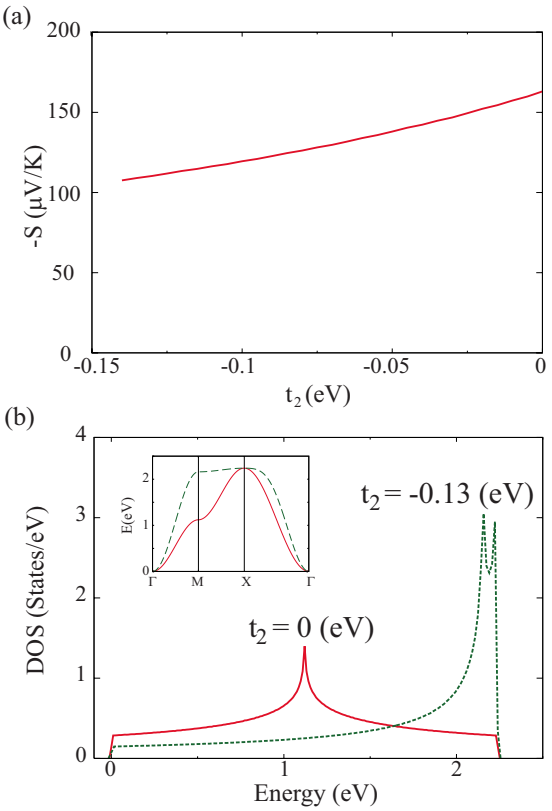

FIG. 4. (Color online) (a) The Seebeck coefficient of the single orbital model for $x=0.017$, $t_1=-0.28$ eV, and $T=300$ K plotted as functions of t_2. (b) The density of states and the band structure at $t_1=-0.28$ eV, $t_2=0$ eV (solid red), and $t_2=-0.13$ eV (dashed green).

TABLE I. t_1, t_2, and $|t_2/t_1|$ obtained from constructing maximally localized Wannier orbitals. In performing the band-structure calculations, we have used the experimentally determined lattice parameters taken from the cited references. For $KTaO_3$, we have obtained t_1 and t_2 by fitting the WIEN2K band structure with a tight-binding model.

	t_1 (eV)	t_2 (eV)	$\lvert t_2/t_1\rvert$
$PbTiO_3$ (Ref. 28)	−0.23	−0.073	0.31
$BaTiO_3$ (Ref. 29)	−0.25	−0.066	0.26
$SrTiO_3$ (Ref. 21)	−0.28	−0.078	0.28
$BaZrO_3$ (Ref. 30)	−0.40	−0.081	0.20
$NaNbO_3$ (Ref. 31)	−0.45	−0.091	0.20
$KTaO_3$ (Ref. 22)	−0.52	−0.094	0.18
$BaMnO_3$ (Ref. 32)	−0.17	−0.067	0.41

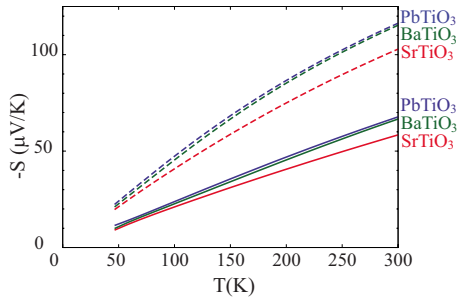

FIG. 5. (Color online) The Seebeck coefficient of $A\mathrm{TiO}_3$(A=Sr,Ba,Pb) at x=0.1 plotted as functions of temperature. The solid lines are obtained using the original effective models while the dashed lines are obtained using models where the bandwidth is halved.

$SrTiO_3$ by about 15% at 300 K. This increase in going from Sr to Ba is qualitatively consistent with the experiments,[34] and it is even in quantitative agreement if we assume that the band width is halved by correlation effects as also shown in Fig. 5 (the experimentally observed Seebeck coefficient is $\sim -120\ \mu\mathrm{V/K}$ at ~ 320 K). On the other hand, $PbTiO_3$ has nearly the same Seebeck coefficient with $BaTiO_3$ because although $|t_1|$ of Pb is smaller than Ba, $|t_2/t_1|$ of Pb is larger, so the two effects nearly cancel each other.

Along this context, we have also evaluated t_1 and t_2 for $KTaO_3$ from the obtained band structure. Although t_1 is much larger compared to that in $SrTiO_3$ as expected from the 5d nature, t_2 is not much changed, and the ratio $|t_2/t_1|$ is the smallest among the materials considered here. In fact, $|t_2/t_1|$ is also small in Zr and Nb compounds, namely, 4d systems with small number of electrons. So it seems that the ratio $|t_2/t_1|$ tends to be small for large principle quantum number. This trend can be considered as another factor working favorable for the thermopower in $KTaO_3$ despite the wide bandwidth.

VI. CONCLUSION

To conclude, we have studied the origin of the large Seebeck coefficient in $SrTiO_3$ and $KTaO_3$. In $SrTiO_3$, from the first-principles band calculation results, a tight-binding model is obtained via the maximally localized Wannier orbitals, and the Seebeck coefficient is calculated using the tight-binding model. In $KTaO_3$, from the first-principles band calculation results, the Seebeck coefficient is calculated using the BOLTZTRAP code. In both materials, the large Seebeck coefficient despite the relatively large conductivity is largely due to the multiplicity of the bands, i.e., essentially the same value of the Seebeck coefficient is obtained for the same number of electrons *per band*, so that when the *total number of doped electrons* itself is the same, the Seebeck coefficient and thus the power factor are larger for multiple band systems. Also, we have examined the effect of the band shape. Although the negative t_2 value is not favorable for the electron doped thermoelectric materials, 4d and 5d systems such as $KTaO_3$ tend to have similar t_2 values as in 3d systems despite the wide bandwidth, and this can be another factor that is advantageous for good thermoelectric properties.

ACKNOWLEDGMENTS

We acknowledge Yasujiro Taguchi for motivating us to start the present study. We also thank Akihiro Sakai and Yoshinori Tokura for sending the preprint on the Ba-doped $KTaO_3$ prior to publication. The numerical calculations were in part performed at the Supercomputer Center, ISSP, University of Tokyo. This work was supported by Grants-in-Aid from MEXT, Japan. H.U. acknowledges support from JSPS.

*Present address: Department of Physics, Tohoku University, Sendai 980-8578, Japan.

[1] I. Terasaki, Y. Sasago, and K. Uchinokura, Phys. Rev. B **56**, R12685 (1997).
[2] S. Li, R. Funahashi, I. Matsubara, K. Ueno, and H. Yamada, J. Mater. Chem. **9**, 1659 (1999).
[3] K. Fujita, T. Mochida, and K. Nakamura, Jpn. J. Appl. Phys. **40**, 4644 (2001).
[4] S. Hébert, S. Lambert, D. Pelloquin, and A. Maignan, Phys. Rev. B **64**, 172101 (2001).
[5] Y. Miyazaki, M. Onoda, T. Oku, M. Kikuchi, Y. Ishii, Y. Ono, Y. Morii, and T. Kajitani, J. Phys. Soc. Jpn. **71**, 491 (2002).
[6] M. Lee, L. Viciu, L. Li, Y. Wang, M. L. Foo, S. Watauchi, R. A. Pascal, Jr., R. J. Cava, and N. P. Ong, Nature Mater. **5**, 537 (2006).
[7] S. Okada and I. Terasaki, J. Appl. Phys. **44**, 1834 (2005).
[8] Y. Okamoto, M. Nohara, F. Sakai, and H. Takagi, J. Phys. Soc. Jpn. **75**, 023704 (2006).
[9] T. Okuda, K. Nakanishi, S. Miyasaka, and Y. Tokura, Phys. Rev. B **63**, 113104 (2001).
[10] H. Ohta, K. Sugiura, and K. Koumoto, Inorg. Chem. **47**, 8429 (2008).
[11] A. Sakai, T. Kanno, S. Yotsuhashi, H. Adachi, and Y. Tokura, Jpn. J. Appl. Phys. **48**, 097002 (2009).
[12] D. J. Singh, Phys. Rev. B **61**, 13397 (2000).
[13] G. B. Wilson-Short, D. J. Singh, M. Fornari, and M. Suewattana, Phys. Rev. B **75**, 035121 (2007).
[14] K. Kuroki and R. Arita, J. Phys. Soc. Jpn. **76**, 083707 (2007).
[15] H. Usui, R. Arita, and K. Kuroki, J. Phys.: Condens. Matter **21**, 064223 (2009).
[16] R. Arita, K. Kuroki, K. Held, A. V. Lukoyanov, S. Skornyakov, and V. I. Anisimov, Phys. Rev. B **78**, 115121 (2008).
[17] W. Koshibae, K. Tsutsui, and S. Maekawa, Phys. Rev. B **62**, 6869 (2000).
[18] W. Koshibae and S. Maekawa, Phys. Rev. Lett. **87**, 236603 (2001).
[19] L. D. Hicks and M. S. Dresselhaus, Phys. Rev. B **47**, 12727 (1993).
[20] For a general review on the theoretical aspects as well as experimental observations of thermopower, see, G. D. Mahan, Solid

State Phys. **51**, 81 (1997).
[21] R. H. Mitchell, A. R. Chakhmouradian, and P. M. Woodward, Phys. Chem. Miner. **27**, 583 (2000).
[22] E. A. Zhurova, Y. Ivanov, V. Zavodnik, and V. Tsirelson, Acta Crystallogr., Sect. B: Struct. Sci. **56**, 594 (2000).
[23] S. Baroni, A. Dal Corso, S. de Gironcoli, P. Giannozzi, C. Cavazzoni, G. Ballabio, S. Scandolo, G. Chiarotti, P. Focher, A. Pasquarello, K. Laasonen, A. Trave, R. Car, N. Marzari, and A. Kokalj, http://www.quantum-espresso.org/; Here we adopt the exchange correlation functional introduced by J. P. Perdew, K. Burke, and Y. Wang, Phys. Rev. B **54**, 16533 (1996), and the wave functions are expanded by plane waves up to a cutoff energy of 60 Ry; 10^3 k-point meshes are used with the special points technique by H. J. Monkhorst and J. D. Pack, *ibid.* **13**, 5188 (1976).
[24] N. Marzari and D. Vanderbilt, Phys. Rev. B **56**, 12847 (1997); I. Souza, N. Marzari, and D. Vanderbilt, *ibid.* **65**, 035109 (2001); The Wannier functions are generated by the code developed by A. A. Mostofi, J. R. Yates, N. Marzari, I. Souza, and D. Vanderbilt, http://www.wannier.org/
[25] P. Blaha, K. Schwarz, G. K. H. Madsen, D. Kvanicka, and J. Luitz, *WIEN2k: An Augmented Plane Wave Plus Local Orbitals Program for Calculating Crystal Properties* (Technische Universität Wien, Austria, 2001).
[26] G. K. H. Madsen and D. J. Singh, Comput. Phys. Commun. **175**, 67 (2006).
[27] There is a flat portion along Γ-X near the bottom of the t_{2g} bands. However, this is not a flat band that induces large DOS, but rather it is simply due to the two-dimensional nature of the d_{yz} band, which has small dispersion in the x direction.
[28] A. M. Glazer and S. A. Mabud, Acta Crystallogr., Sect. B: Struct. Crystallogr. Cryst. Chem. **34**, 1065 (1978).
[29] R. D. King-Smith and D. Vanderbilt, Phys. Rev. B **49**, 5828 (1994).
[30] S. Yamanaka, M. Fujikane, T. Hamaguchi, H. Muta, T. Oyama, T. Matsuda, S. Kobayashi, and K. Kurosaki, J. Alloys Compd. **359**, 109 (2003).
[31] S. P. Solov'ev, Y. N. Venevtsev, and G. S. Zhdanov, Kristallografiya **6**, 218 (1961).
[32] *Review on Chemistry* No. 32, edited by Japanese Chemical Society (in Japanese).
[33] A similar cation dependence of the transport properties has been discussed for the clathrates in G. K. H. Madsen, K. Schwarz, P. Blaha, and D. J. Singh, Phys. Rev. B **68**, 125212 (2003).
[34] H. Muta, K. Kurosaki, and S. Yamanaka, J. Alloys Compd. **368**, 22 (2004).